Scaling and dynamics of large-scale structures in turbulent boundary layers with pressure gradients

Felix Eich

Institute of Fluid Mechanics and Aerodynamics
Universität der Bundeswehr München
Werner-Heisenberg-Weg 39
85577 Neubiberg, Germany
Felix.Eich@unibw.de

Christian J. Kähler

Institute of Fluid Mechanics and Aerodynamics
Universität der Bundeswehr München
Werner-Heisenberg-Weg 39
85577 Neubiberg, Germany
Christian.Kaehler@unibw.de

ABSTRACT

This paper describes the experimental investigation of large-scale structures in turbulent boundary layers with particle image velocimetry (PIV). The objective of the measurements was to determine the influence of the Reynolds number and pressure gradient on the topology, size and spatial distribution of large-scale structures. Using multiple PIV systems aligned side by side, it was possible to capture the full spatial extend of large-scale structures for a friction velocity Reynolds number range between $Re_\tau = 4200 - 13400$. The measured velocity fields were analysed by statistical multi-point methods to determine the average structure sizes, shape and spacing of the large scale turbulent structures in several wall-parallel measurement planes and in a plane normal to the mean flow direction. Conditioning the statistical analysis on low and high momentum fluid events shows distinct changes in the shape and size of the coherent flow structures. The application of quadrant analysis in combination with conditioned correlation analysis on the data sets, made it possible to identify a connection between large-scale structures with specific high turbulent kinetic energy and characteristic Q2 and Q4 events.

Introduction

The investigation of coherent flow structures in turbulent boundary layers has been subject to intensive research over the past decades, indicated in the references listed in the review by Wallace (2012). However, the instantaneous spatial organisation of large-scale coherent structures and their statistical impact on the turbulent mixing is still under debate. Investigating large-scale structures experimentally is difficult due to their size, which can extend multiple boundary layer thicknesss in length (Dennis & Nickels, 2011). Another difficulty is the need for high Reynolds numbers, because the larger the Reynolds number the better the structures can be detected (Hutchins & Marusic, 2007b).

Tomkins & Adrian (2003) performed wall parallel PIV measurements and showed that large-scale structures align in a streaky pattern, comparable to near-wall streaks in the boundary layer (Smith & Metzler, 1983), but scale in much larger dimensions. To characterize the topological features of these structures and their spatial organisation, large field PIV measurements were performed in order to capture the structures in their full spatial extent. Buchmann *et al.* (2016) have shown that large-scale high-resolution investigations are possible even at high Reynolds numbers with multi-camera recording and sophisticated PIV / PTV evaluation techniques. However, in the present experiment this requires a constant light-sheet thickness all over the full field of view. Hain *et al.* (2016) have shown that an almost constant light sheet thickness of about 1 mm over 3 m length can be obtained if long focal length lenses are used and the distance between the lenses and the measurement plane is sufficiently large. Using multiple statistically independent PIV images it is possible to perform multi-point statistical analysis and thereby analyse characteristic structure patterns quantitatively. The results of Buchmann *et al.* (2016) showed that the size of the structures is independent of the Reynolds number if scaled with the boundary layer thickness. Moreover, they showed that the length of the turbulent large scale structures raises with the magnitude of the turbulent velocity fluctuations. Low and high momentum superstructures are significantly elongated with respect to the superstructures convecting with the mean velocity of the flow according to the analysis. In addition the topology of the turbulent structures in the stream-wise wall-normal plane depends strongly on the momentum of the turbulent structures. This indicates that the superstructures are not universal, rather they exist in different forms.

So far, the majority of studies on turbulent boundary layer research have focused on zero-pressure gradient (ZPG) canonical flows, e.g. flat plate turbulent boundary layers. However, nearly all technical flows are subject to pressure gradients, especially in aerodynamics. Previous experiments showed that pressure gradients have an influence on large-scale structures (Harun *et al.*, 2013; Reuther *et al.*, 2015; Hain *et al.*, 2016). The turbulent kinetic energy transported with the large-scale structures is significantly increased and the length-scales are reduced under the influence of an adverse pressure gradient (Reuther *et al.*, 2015). This motivated the present study, where the scaling and dynamics of large-scale structures under the influence of an adverse pressure gradient are analysed and compared to a zero pressure gradient flow.

In the following sections, the setup and results of several PIV measurements in wall-parallel planes and planes normal to the mean flow direction with and without a pressure gradient are presented and discussed. The coordinates x, y and z correspond to stream-wise, wall-normal and span-wise directions, u, v and w to the respective velocity components. Temporally averaged values are indicated with an overbar ($\overline{u}$), fluctuations with a dash (u'). The superscript "+" refers to viscous scaled units.

Experimental Setup

The experiments were conducted in the Atmospheric Wind Tunnel Munich (AWM), which is an Eiffel-Type wind tunnel at the Bundeswehr University Munich. The wind tunnel has a 22 m test section with a cross section of $1.85 \times 1.85\,\mathrm{m}^2$. As the boundary layer thickness is about 10 times smaller than the wind tunnel width no influence from the opposite wind tunnel wall or from the corner vortices is expected according to Jones *et al.* (1995). Approximately 5 m downstream of the settling chamber, a 7 m long boundary layer model is installed in the wind tunnel side wall. The model consists of two S-shape deflections with a 4 m flat plate section in between. In order to investigate different pressure gradients, the model was designed with a zero pressure gradient over the flat plate section and a well defined adverse pressure gradient $\mathrm{d}p/\mathrm{d}x > 0$ at the expanding S-shape deflection. A 3D sketch of the boundary layer model with an example Stereo-PIV (SPIV) setup is shown in figure 1. In figure

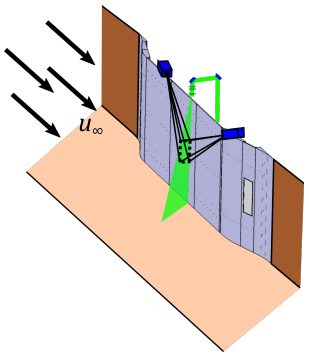

Figure 1. 3D sketch of the boundary layer model installed in the wind tunnel sidewall. Over the flat plate ZPG part, an example Stereo-PIV setup is shown.

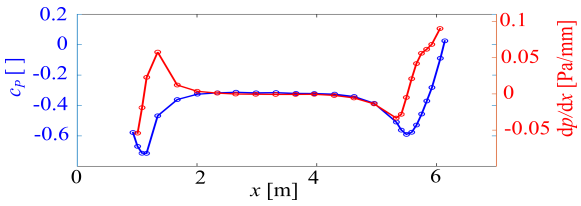

Figure 2. Pressure distribution over the boundary layer model at $Re_\tau = 4200$. $x = 0$ corresponds to the beginning of the boundary layer model. The blue line shows the pressure coefficient c_p, the red line the pressure gradient $\mathrm{d}p/\mathrm{d}x$.

2, the resulting pressure distribution at $Re_\tau = 4200$ is plotted. Clearly visible is the zero pressure gradient above the flat plate section and the adverse pressure gradient on the downstream end of the model. Having a boundary layer development length of approximately 10 m before the measurement location results in a fully developed turbulent boudary layer with a thickness of 140 mm in the ZPG region. Therefore, it is possible to investigate the influence of the wall distance on large-scale structures even in wall-parallel planes, because the light sheet thickness d_L is small compared to the boundary layer thickness δ.

PIV Measurement Parameters

To investigate the influence of the Reynolds number, a range of $Re_\tau = 4200 - 13400$, calculated at the end of the ZPG position, was selected for the measurements. This is above the lower limit of $Re_\tau \geq 1700$ given by Hutchins & Marusic (2007a) for a definite scale separation for the detection of large-scale structures in turbulent boundary layer energy spectra. Due to the spatial extension of large-scale structures, multiple PIV systems aligned adjacently in the stream-wise direction were used to capture an adequate spatial domain. The utilisation of multiple systems is necessary, because large-scale structures easily exceed 1 m in length for a boundary layer thickness of 140 mm. In both, the ZPG and APG parts of the boundary layer model, PIV investigations in wall-parallel planes at wall distances of $y/\delta = 0.07,\ 0.14,\ 0.28$ and 0.55 were measured. To get a further insight in the topology of large-scale structures, additional SPIV measurements were performed in wall-normal planes perpendicular to the main flow direction. The illumination for this investigation was generated by an Innolas Spitligth Nd:YAG (140 mJ/pulse) and a Spectra Physics laser (400 mJ/pulse) for wall-normal and wall-parallel measurements, respectively. Tracer particles made from DEHS with Laskin nozzle seeders were added to the flow in the wind tunnel inlet tower. The average particle diameter is approximately 1 μm (Kähler *et al.*, 2002). For the ZPG Stereo and APG measurements a local seeding system was used where only the turbulent part of the boundary layer is seeded. Using a proper masking function based on the seeding distribution, it was possible to analyse a turbulent boundary layer while avoiding bias errors of the turbulent structure statistics due to laminar entrainment. To ensure convergence and being able to calculate statistics of large-scale structures, at least 10000 statistically independent images were taken per measurement location. The PIV images were analysed with the commercial software DaVis from LaVision. Using a multi-pass algorithm with 50 % interrogation window overlap, resulting vector spacings between 0.8 mm – 2.7 mm were achieved. In table 1 the resulting flow parameters calculated from the vector fields are given.

Table 1. Flow parameters of the PIV measurements.

u_∞	$Re_{\tau,\mathrm{ZPG}}$	$u_{\tau,\mathrm{ZPG}}$	δ_{ZPG}	$u_{\tau,\mathrm{APG}}$	δ_{APG}
m/s		m/s	m	m/s	m
10	4200	0.45	0.145	0.22	0.21
23	9300	0.98	0.148	0.53	0.22
36	13400	1.45	0.142	0.88	0.21

Results and Discussion

The most intuitive way to get a first idea of the spatial pattern of large-scale structures in turbulent boundary layers is to look on instantaneous fields of the velocity fluctuations measured in a wall-parallel plane (Kähler *et al.*, 1998). In upper plot of figure 3, an instantaneous snapshot of the velocity fluctuations in stream-wise direction at $Re_\tau = 9300$ in the log layer is shown. The contours correspond to the normalised velocity fluctuations $u'/\overline{u}$. Clearly identifiable are regions of high (red) and low (blue) momentum fluid within the flow aligned in a streaky pattern side by side. Due to the remarkable large field of view of $10\delta \times 3\delta$, several large-scale structures which extend multiple boundary layer thicknesss δ in length can be found. However, assigning discrete values for the structure length is difficult due to the strong variation of the length and width of the structures, but also because a cut through the structures at a specific wall distance only gives a partial view and not the total length L_1 of the structure, which is much longer according to Buchmann *et al.* (2016). Therefore, the vector fields are analysed by means of two-point spatial correlation of the velocity fluctuations to determine average structure sizes and spacings in the specific measurement plane. In the following, the average length of the structures in the cut-plane will be referred as L_2, the width as W_2 respectively. The difference between the total length L_1 and the length in the cut-plane L_2 illustrated out in figure 4 for an exemplary large-scale structure. In the following sections, the structure size and spacing based on the results from the analysis of the acquired vector fields by means of two-point correlations will be discussed. The correlation function R_{uu} for a chosen correlation point P is defined as

$$R_{uu}(x,y,z) = \frac{\sum u'(x,y,z) \cdot u'(x_\mathrm{P},y_\mathrm{P},z_\mathrm{P})}{N \cdot \sigma_u(x,y,z) \cdot \sigma_u(x_\mathrm{P},y_\mathrm{P},z_\mathrm{P})}, \qquad (1)$$

with the standard deviation of the velocity component $\sigma_u(x,y,z)$ and the number of independent fields N. In figure 3, the velocity fluctuations and the corresponding correlation coefficient at $y/\delta = 0.14$

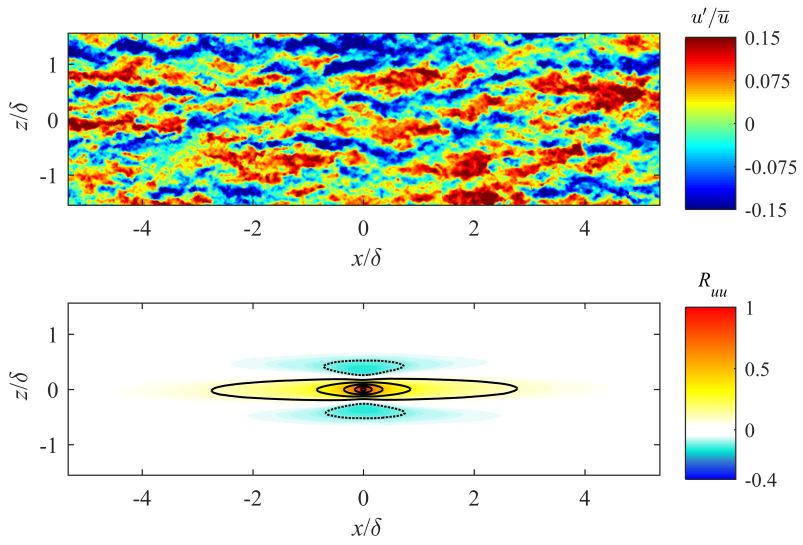

Figure 3. Top: Instantaneous normalised velocity fluctuation $u'/\overline{u}$ at $Re_\tau = 9300$ and a wall distance $y/\delta = 0.14$ with zero pressure gradient. Positive values (red) indicate high momentum fluid, negative values are low momentum fluid (blue). Bottom: Resulting two-point correlation plane. Contour lines from 0.1 to 0.9 in steps of 0.2. Solid lines mark positive correlated areas, dotted contour lines stand for negative correlation. The distance between the two minima (blue) is equal to the structure periodicity λ as defined in figure 6 and visible in figure 7 top.

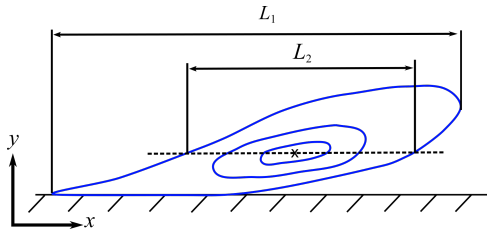

Figure 4. Sketch of the spatial correlation function, indicating the mean size and shape of large-scale structure (blue) in the xy-plane. Total structure length L_1 and structure length L_2 in a cut-plane are shown. The dashed line represent the measurement plane of the wall-parallel measurements.

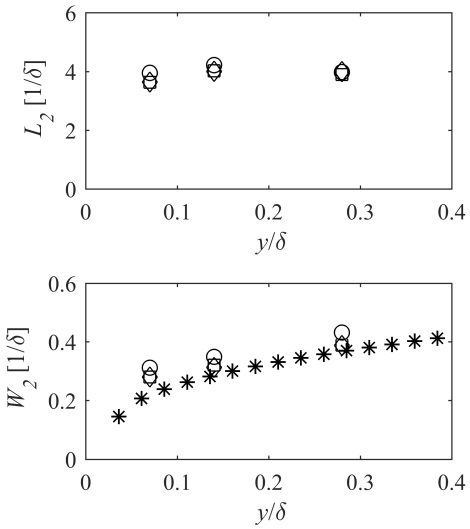

Figure 5. Resulting large-scale structure length (top) and width (bottom) in a turbulent boundary layer flow with zero pressure gradient (ZPG) calculated from two-point correlation functions with a threshold of $R_{uu} = 0.15$. Symbols correspond to different Reynolds numbers measured in the wall-parallel $xz-$plane: $\diamond$, $Re_\tau = 4200$; $\square$, $Re_\tau = 9300$; o, $Re_\tau = 13400$. The $*$-symbols correspond to Reynolds numbers $Re_\tau = 9300$ measured in the cross-stream $yz-$plane.

are shown. The centre of the correlation field, indicated by the positive correlated region, visualizes the size and shape of coherent flow structures. Clearly visible is the strong stretching in stream-wise direction and the small span-wise extend. The average elongated flow structure in stream-wise direction, flanked by two negative correlated areason both sides of the elongated structures indicate the span-wise alternation between high and low momentum structures. The comparison with the instantaneous field of the velocity fluctuations shows that the distance between the two negative peaks correlates with the separation between low momentum structures.

Scaling with wall distance and Reynolds number

In figure 5 top, the resulting large-scale structure length and in the bottom plot the width calculated from correlation planes of the ZPG turbulent boundary flow measurements are shown. To calculate structure length and width from the correlation planes, a threshold of $R_{uu} = 0.15$ was chosen. This threshold is well above the PIV uncertainty and the calculated correlated length and width can be assumed to be independent of random noise.

As stated by Hutchins & Marusic (2007b) and proven by Buchmann *et al.* (2016) as well, the length L_2 of large-scale structures is relatively constant about 4δ for a wide range of Reynolds numbers and wall distances. Both is in good agreement with this study. The use of different thresholds for R_{uu} results in discrepancies of the absolute measured length L_2. There is a slight maximum of the structure length at $y/\delta = 0.14$, but otherwise the influence of the wall distance is minimal. Maxima of the length L_2 were observed around $y/\delta = 0.15 - 0.25$ in previous PIV experiments as well (Reuther *et al.*, 2015; Buchmann *et al.*, 2016).

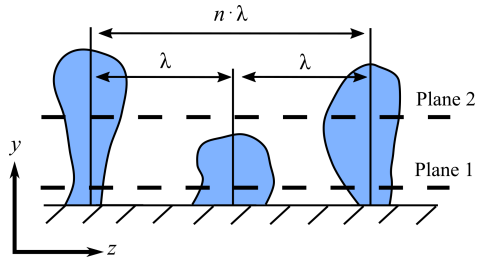

Figure 6. Sketch of turbulent structures (blue) with different shape and different wall-normal extension analysed in two wall-parallel planes. The span-wise spacing at the wall λ is constant for all structures.

In contrast to the length, there is an increase of the average width W_2 with the wall distance y as shown in figure 5 bottom. The growth in structure size with increasing wall distance is can be qualitatively explained using Townsend's attached eddy hypotheses (Townsend, 1976). However, an even simpler, more consistent and more physical based explanation for the structure growth follows from the impact of varying structure heights on the statistical multi-point analysis. If large-scale turbulent structures with varying wall-normal heights but a nearly constant span-wise spacing λ are analysed in a wall-parallel plane, as shown in figure 6, the variation of structure height results statistically in an increased correlated width. The variation in discrete structure steps $n \cdot \lambda,\ n \in \mathbb{N}$ can be found in all instantaneous snapshots of the wall-parallel plane and wall-normal plane measurements, highlighted exemplary in figure 7 and supports the previous statistical explanation which only assumes a statistical variation of the large scale structure in y direction. This variation follows naturally from the shape of the correlation function indicated in figure 4. However, to further validate this explanation measurements in a plane normal to the mean flow direction were performed. The result shown in the lower image of figure 7 confirms the assumption of the hight variation of the large scale structures.

Dynamics of turbulent structures

Understanding the dynamics of turbulent structures is crucial for the understanding of production and transport processes within a turbulent boundary layer. Hutchins & Marusic (2007a) found by means of hot wire measurements, that large-scales have an effect on the near wall flow structures and modulate the near wall cycle. Investigations of Buchmann *et al.* (2016) show a strong correlation between turbulent large-scale structures and the wall pressure fluctuations. This confirms directly that the large-scale structures have an impact down to the wall. Furthermore, they could demonstrate that large-scale structures can vary strongly in the magnitude of the turbulent fluctuations and they revealed significant topological difference between high and low momentum large-scale structures. To prove if there is a connection between the large-scale structures and characteristic events in the turbulent boundary layer, known as Q2 and Q4 events where $u'v' \ll 0$, the quadrant analysis (Wallace, 2016) was applied. In figure 8, the joint probability density distribution of the velocity fluctuations u' and v' at $Re_\tau = 9300$ and a wall distance $y/\delta = 0.16$ is plotted. The quadrants Q2 and Q4, which indicate flow events producing negative Reynolds shear stresses $u'v' < 0$, are clearly over represented in the upper part of the log-layer. To analyse the characteristic structures, which are associated with the Q2 and Q4 events and to calculate their size and alignment, the flow fields have to be conditioned on appropriate events. One possible criterion to condition the data sets on flow events is the turbulent fluctuation in streamwise direction u', where inside a Q2 event, $u' < 0$ (low momentum structure) and within a Q4 event $u' > 0$ (high momentum structure). The final conditioning criterion used in this study is based on the standard deviation σ_u of the velocity u. For the analysis, only flow events where $u' > k \cdot \sigma,\ k = 1,\ 1.5,\ 2$ in case of a Q4-event and $u' < -k \cdot \sigma,\ k = 1,\ 1.5,\ 2,\ 2.5$ in case of a Q2-event are correlated.

In figure 9, the calculated width and length from the conditioned correlation analysis are plotted based on the measurements from the cross-stream plane. In accordance with Buchmann *et al.* (2016), the correlated structure length increases for high and low momentum structures. Furthermore, the measurements presented here show again that the width of the structures vary with the wall distance due to the statistical height of the large scale structures but interestingly, the width is independent on the magnitude of the negative velocity fluctuations. This holds even true for extreme seldom events revealing very large negative velocity fluctuations.

Another interesting aspect of conditioned correlations is the physical consequence in terms of energy. The increase of the average structure length in the two-point correlations with conditioning on higher turbulent kinetic energy points out that large-scale structures are associated with high kinetic energy within the turbulent boundary layer as found before by Hutchins & Marusic (2007a) based on hot-wire measurements. They demonstrated, using premultiplied energy spectra that an outer peak occurs at $y/\delta = 0.06$. They estimated the streamwise wave-number λ_x connected to this energy peak is approximately $\lambda_x = 6\delta$. This is within the same magnitude as the structure length calculated from PIV measurements and two-point correlations, as shown in figure 9. Therefore, the findings of Hutchins & Marusic (2007a) are nicely confirmed with an independent measurement that in addition does not require the assumption of Taylor's hypothesis.

Effect of pressure gradient on the scaling of large-scale structures

To investigate the influence of the pressure gradient on the scaling of the large-scale structures, measurements were performed in the APG section of the boundary layer model which is located downstream at the second S-shape deflection. In figure 10 two examples of the flow field at $Re_\tau = 9300$ are shown. The Reynolds number correspond to the number calculated at the ZPG. Comparing the APG case in figure 10 and the ZPG cases of figures 3 and 7, the streaky patterns of correlated velocity fluctuations can be found as well under the influence of an APG. Figure 10 left shows a strong increase of the normalised streamwise velocity fluctuation from left to right. This is a result of two effects: First, the reduced mean velocity and second, the increase in turbulent activity due to the positive pressure gradient. Taking only high (red) and low (blue) momentum zones into account in figure 10, the pattern neither changes in size nor in alignment with increasing APG. This presumes, that the large-scale structures survive under the action of a pressure gradient. To compare quantitatively structure sizes, the flow fields from the adverse pressure gradient measurements are analysed by two-point correlations as well. Due to the smaller field of view in streamwise direction, a higher threshold for the length calculation is necessary. Hence, a threshold of $R_{uu} = 0.4$ is used. The resulting width, length and a comparison with the ZPG results is shown in figure 11. As expected, the large-scale structure length is decreasing under the influence of an adverse pressure gradient. Similar observations were made by Harun *et al.* (2013). In their experimental studies, they showed that the peak in the premultiplied energy spectra moves from wavelength $\lambda_x/\delta \approx 4$ in the ZPG to $\lambda_x/\delta \approx 3$ in the APG. In this experimental study, the shortening is even more pronounced. Comparing the large-scale structure width, the struc-

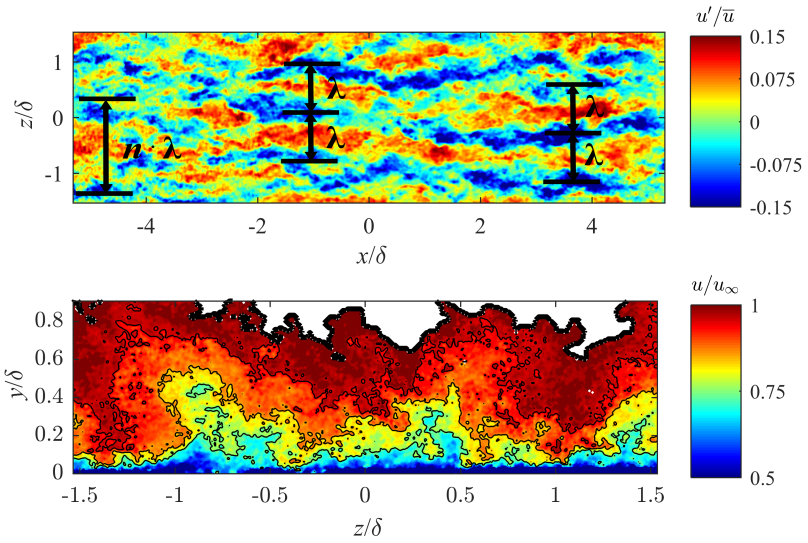

Figure 7. Top: Instantaneous normalised velocity fluctuation $u'/\overline{u}$ at $Re_\tau = 9300$ and a wall distance $y/\delta = 0.28$ with zero pressure gradient. The structure spacing λ and multiple spacings $n \cdot \lambda$ in span-wise direction are indicated. Bottom: Instantaneous normalised velocity u/u_∞ in a cross-stream yz-plane. Laminar parts (white) are masked out via the seeding concentration. Contour lines correspond to $u/u_\infty = 0.75,\ 0.85$ and 0.95.

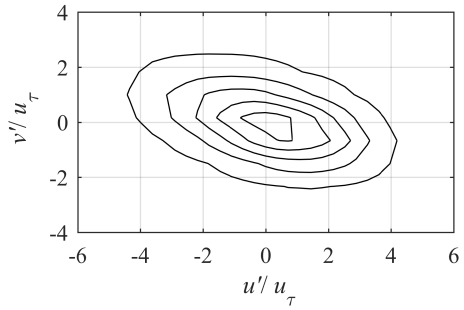

Figure 8. Joint probability distribution of the fluctuations u' and v' at a wall distance $y/\delta = 0.16$ and Reynolds number $Re_\tau = 9300$ in the ZPG turbulent boundary layer.

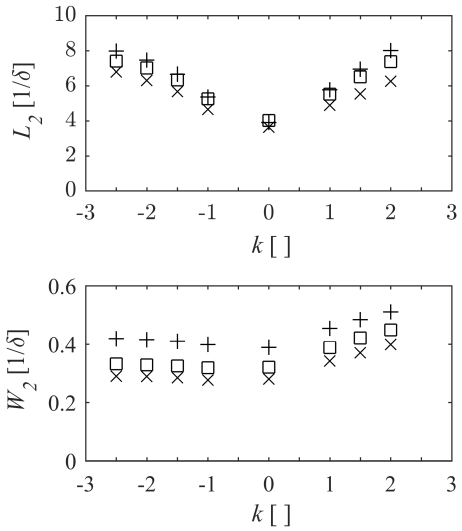

Figure 9. Turbulent structure length (top) and width (bottom) from conditioned two-point correlations in the ZPG, threshold $R_{uu} = 0.15$. Symbols correspond to different wall distances: $+$, $y/\delta = 0.28$; $\square$, $y/\delta = 0.14$; $\times$, $y/\delta = 0.07$.

tures are growing again with increasing wall distance. For all cases in the APG, there is no influence of the Reynolds number on the size of large-scale structures. The boundary layer thickness increases from $\delta_{\mathrm{ZPG}} \approx 0.145\,\mathrm{m}$ to $\delta_{\mathrm{APG}} \approx 0.21\,\mathrm{m}$, which is an increase of approximately 45 % in boundary layer thickness. The physical length of the large-scale structures decreases by $49-69\,\%$. A different behaviour is observed in the width scaling. For a wall distance of $y/\delta = 0.07$, the absolute structure spacing is smaller in the APG than in the ZPG, for $y/\delta = 0.14$ the spacing is nearly similar whereas for $y/\delta = 0.28$ the distance between the structures is increased in the APG. Another indicator, that there is a change in the structure behaviour with the wall distance under an APG influence is the point of inflexion in the slope of the structure width at approximate $y/\delta = 0.18$, visible in the APG stereo PIV measurements ($yz-$plane) in figure 11. One possible explanation is the existence of two large-scale structures regimes. The inner structures are newly produced or strongly modulated in the APG region, whereas the large-scale structures further away from the wall originate from the ZPG part of the boundary layer. They are convected in the APG part without significant adaptation to the APG conditions.

Conclusions

Large field of view PIV measurements were conducted to detect and analyse large-scale coherent structures in turbulent boundary layers with and without pressure gradient. Comparing instantaneous flow fields demonstrated a characteristic streaky nature of the meandering large scale turbulent flow structures. A statistical analysis shows that the length of the large-scale structures in the measurement plane is relatively constant but the width of large-scale structures increases with the wall distance. This could be explained by the natural height variation of the large-scale structures.

Conditioning the structure analysis on high and low momentum flow events, an increase in large-scale structure length up to 8δ

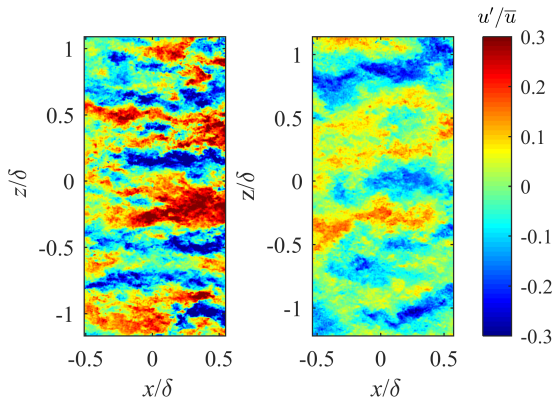

Figure 10. Instantaneous normalised velocity fluctuation fields $u'/\overline{u}$ in wall parallel planes at $Re_\tau = 9300$ under the influence of an adverse pressure gradient. Left: Wall distance $y/\delta = 0.14$, right: $y/\delta = 0.28$.

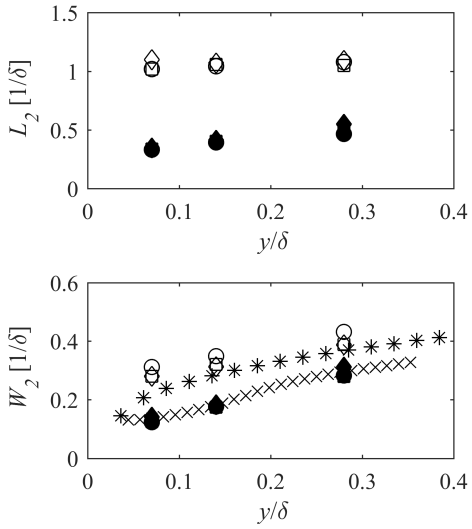

Figure 11. Comparison of ZPG (open symbols) and APG (filled symbols) large-scale structures length (top) and width (bottom) at different wall positions. Symbols correspond to different Reynolds numbers measured in the wall parallel $xz-$plane: $\diamond$, $Re_\tau = 4200$; $\square$, $Re_\tau = 9300$; o, $Re_\tau = 13400$. The $*$-symbols correspond to Reynolds numbers $Re_\tau = 9300$ measured in the cross-stream $yz-$plane in the ZPG, $\times$-symbols to the APG case.

with increasing turbulent kinetic energy was found. Interestingly, the structure spacing stayed nearly constant for low momentums structures while increasing as well for high momentum structures with increased turbulent kinetic energy. Furthermore, a comparisons of the conditioned correlations with quadrant analysis showed, that significantly elongated large-scale structures are associated with the characteristic Q2 and Q4 events and therefore connected with high stress production.

Finally, influence of an APG was tested and compared to the ZPG canonical boundary layer flow. As expected from previous investigations (Harun *et al.*, 2013; Reuther *et al.*, 2015), the large-scale structures are shorter in streamwise direction. Comparison of the structure width and estimation of the effect due to scaling with an increased boundary layer thickness, suggested the existence of two different large-scale structure regimes closer to the wall $y < 0.18\delta$ and further outside.

Acknowledgements

The authors would like to thank the Deutsche Forschungsgemeinschaft (DFG) for the financial support via the project "Analyse turbulenter Grenzschichten mit Druckgradient bei großen Reynolds-Zahlen mit hochauflsenden Vielkameramessverfahren" (KA1808/14 – 2).

REFERENCES

Buchmann, N. A., Kücükosman, Y. C., Ehrenfried, K. & Kähler, C. J. 2016 Wall pressure signature in compressible turbulent boundary layers. In *Progress in Wall Turbulence 2*, pp. 93–102. Springer.

Dennis, D. J. C. & Nickels, T. B. 2011 Experimental measurement of large-scale three-dimensional structures in a turbulent boundary layer. part 2. long structures. *Journal of Fluid Mechanics* **673**, 218–244.

Hain, R., Scharnowski, S., Reuther, N., Kähler, C. J., Schröder, A., Geisler, R., Agocs, J., Röse, A., Novara, M., Stanislas, M. *et al.* 2016 Coherent large scale structures in adverse pressure gradient turbulent boundary layers. In *18th IInternational Symposia on Applications of Laser Techniques to Fluid Mechanics, 04. - 07. July. 2016, Lisbon, Portugal*.

Harun, Z., Monty, J. P., Mathis, R. & Marusic, I. 2013 Pressure gradient effects on the large-scale structure of turbulent boundary layers. *Journal of Fluid Mechanics* **715**, 477–498.

Hutchins, N. & Marusic, I. 2007a Large-scale influences in near-wall turbulence. *Phil Trans. of the Royal Soc. A.: Mathematical, Physical and Engineering Sciences* **365** (1852), 647–664.

Hutchins, N. & Marusic, I. 2007b Evidence of very long meandering features in the logarithmic region of turbulent boundary layers. *Journal of Fluid Mechanics* **579**, 1–28.

Jones, M. B., Marusic, I. & Perry, A. E. 1995 The effect of aspect ratio and divergence on the turbulence structure of boundary layers. In *Proceedings, 12th Australasian Fluid Mechanics Conference*.

Kähler, C. J., Adrian, R. J. & Willert, C. E. 1998 Turbulent boundary layer investigations with conventional and stereoscopic particle image velocimetry. In *9th International Symposium on Applications of Laser Techniques to Fluid Mechanics, 13. - 16. July. 1998, Lisbon, Portugal*.

Kähler, C. J., Sammler, B. & Kompenhans, J. 2002 Generation and control of tracer particles for optical flow investigations in air. *Experiments in fluids* **33** (6), 736–742.

Reuther, N., Schanz, D., Scharnowski, S., Hain, R., Schröder, A. & Kähler, C. J. 2015 Experimental investigation of adverse pressure gradient turbulent boundary layers by means of large-scale piv. In *11th International Symposium on Particle Image Velocimetry - PIV15 -, 14. - 16. Sept. 2015, Santa Barbara, CA, USA*.

Smith, C. R. & Metzler, S. P. 1983 The characteristics of low-speed streaks in the near-wall region of a turbulent boundary layer. *Journal of Fluid Mechanics* **129**, 27–54.

Tomkins, C. D. & Adrian, R. J. 2003 Spanwise structure and scale growth in turbulent boundary layers. *Journal of Fluid Mechanics* **490**, 37–74.

Townsend, A. A. 1976 *The structure of turbulent shear flow*. Cambridge university press.

Wallace, J. M. 2012 Highlights from 50 years of turbulent boundary layer research. *Journal of Turbulence* **13**, N53.

Wallace, J. M. 2016 Quadrant analysis in turbulence research: history and evolution. *Annual Review of Fluid Mechanics* **48**, 131–158.